Access to hole dynamics in graphite by femtosecond luminescence and photoemission spectroscopy

Tohru Suemoto, Shigeyuki Sakaki, Makoto Nakajima, Yukiaki Ishida, and Shik Shin
ISSP, University of Tokyo, Kashiwa-no-ha, Kashiwa, Chiba 277-8561, Japan
(Received 19 December 2012; revised manuscript received 27 April 2013; published 10 June 2013)

Ultrafast dynamics of holes in a solid is usually hard to observe directly because the optical transition includes both electron and hole dynamics. In this paper we show an approach combining femtosecond luminescence and photoemission spectroscopy, successfully applied to graphite. Ultrafast infrared luminescence is observed in graphite and ascribed to recombination luminescence, though graphite is a semimetal. The dynamics of holes is deduced by taking a ratio between the time-resolved luminescence and photoemission data recorded on the same sample, and shown to be very close to that of electrons.

DOI: 10.1103/PhysRevB.87.224302 PACS number(s): 78.66.Tr, 78.47.J−, 78.55.Hx, 79.60.Bm

I. INTRODUCTION

Carrier dynamics in solids is an important issue for understanding the light emission process, transport of high momentum carriers, relaxation from the excited electronic states, and energy dissipation channels. It is also relevant to developing high-speed electronic and photonic devices. Traditionally, the ultrafast phenomena in solids have been studied by means of transient absorption, reflection, luminescence, and various nonlinear optical processes. Although these methods are powerful and widely applicable, one cannot avoid mixing up of the information from electrons and holes, because the process includes optical transition within the electronic band structure of the solid. On the other hand, photoemission spectroscopy has an advantage to capture directly the electron population, since single electron excitation spectra are recorded. Owing to this unique property, time-resolved photoemission spectroscopy (TrPES) is recognized as a powerful tool to investigate the carrier dynamics around the Fermi level (E_F).[1–3] Practically, however, the details of the hole dynamics are less accessible than those of the electrons, because the depression of the finite photoemission signal from the occupied states has lower signal-to-noise ratio than the transient signal increase from the states above E_F. Moreover, it is often noticed that the spectral weight across E_F is not conserved,[4,5] which may indicate that the quantum efficiency of photoemission (matrix element) exhibits energy-dependent change in nonequilibrium. It is therefore imperative to combine various ultrafast probes for revealing the whole picture of the carrier dynamics, especially that of holes.

In this paper, we report the ultrafast carrier dynamics of graphite investigated by femtosecond luminescence spectroscopy and TrPES. From the high-speed electronics point of view, graphite as well as graphene[6–8] are promising device materials, since they have conelike massless dispersion centered at the K point in the Brillouin zone projected on surface[9,10] [Fig. 1(a)]. As the dispersion is nearly linear without a band gap, we can expect quite different carrier dynamics compared to that in ordinary semiconductors. Motivated by the importance of the ultrafast response of these systems in applications, the carrier dynamics have been studied by various methods, such as photoemission spectroscopy (PES),[11,12] transient absorption,[13] and terahertz[14] spectroscopy. Anti-Stokes radiation in graphene under femtosecond pulse excitation has also been reported and the time response has been studied with a correlated luminescence signal under double pulse excitation.[15] In spite of these efforts, the hole dynamics has not been extracted experimentally, and symmetry is often assumed for the dynamics of electrons and holes *a priori* in analyzing the experimental data. However, the carrier-phonon interaction via deformation potential is not necessarily the same for the electrons and holes in the π and π^* bands, respectively. Firstly, we report observation of recombination-type luminescence typical for semiconductors in graphite, although graphite is a semimetal. Secondly, through the fact that photoemission and luminescence correspond to upward and downward transitions, respectively, from the same electronic state in the unoccupied band [Fig. 1(a)], we extract the hole dynamics by combining the luminescence and TrPES data.

II. EXPERIMENT

Measurements of the femtosecond luminescence were performed with the up-conversion technique, which enables direct observation of ultrafast luminescence over a wide energy window in the visible-to-infrareds. The apparatus is almost the same as that used in our previous works on wave-packet spectroscopy.[16–18] The sample was excited with amplified mode-locked pulses from a regenerative amplifier operating at a repetition rate of 200 kHz. The wavelength was 790 nm (1.57 eV) and the pulse width was 70 fs. The average power at the sample surface ranged from 10 to 60 mW. The spot size was about 150 μm and the corresponding maximum fluence per pulse was estimated to be 1.7 mJ/cm^2.

Paraboloidal mirrors were used to collect and to refocus the luminescence onto a nonlinear-optical crystal, lithium iodate (LIO). The luminescence light was frequency mixed in the LIO crystal with variably delayed 790 nm pulses from the amplifier. The up-converted signal was spectrally and polarization filtered by an edge filter, a Gran-Taylor prism, and directed to a double grating monochromator (SPEX 1680B) equipped with a cooled photomultiplier tube (Hamamatsu R943-02) and a photon counting system. The system had a sensitivity between 0.23 and 1.3 eV for the luminescence photons. The spectral sensitivity of the up-conversion measuring system was calibrated with a tungsten standard lamp between 0.6 and 1.2 eV. In spite of relatively large spot size on the sample, we realized a time resolution of 150 fs. We used a cleaved surface of a highly oriented pyrolytic graphite (HOPG) block as a sample.

 ©2013 American Physical Society

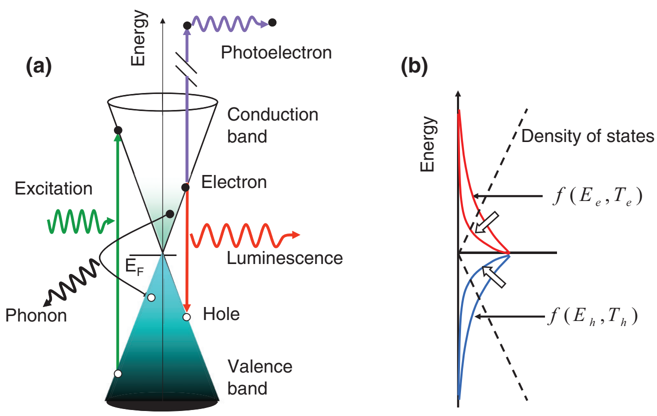

FIG. 1. (Color online) (a) Illustrated are the Dirac-cone band structures near the K point, with photoemission and recombination luminescence processes in graphite. Electron-hole pairs are created by pumping light (upward green arrow; around 1.5 eV) and recombine to give a short-lived luminescence (downward red arrow). When the second pulse (5.9 eV) is impinged, the hot electrons are excited above vacuum level to give photoelectrons. The electron-hole pairs can recombine also by emitting phonons (curved black arrow). (b) Density of states of electrons and holes (dashed black lines), and Fermi-Dirac distribution for electron (red curves) and hole (blue curves) systems. The white arrows show the change of distribution due to cooling process.

All luminescence measurements were performed at room temperature in air.

TrPES measurements were performed with 1.48 eV pumping pulses and 5.9 eV probe pulses at a repetition frequency of 250 kHz, using a setup described in Ref. 12. The angle-integrated PES signal was detected by a hemispherical analyzer. The overall time resolution was 400 fs. The fresh sample surface was prepared by cleaving the sample in vacuum without a heat treatment.

III. RESULTS AND DISCUSSION

In spite of the semimetallic nature of graphite, we have observed moderately strong ultrafast luminescence in the femto-to-picosecond regime, while time-averaged brightness is very low, as the lifetime is short. Figure 2(a) shows the time evolution curves of the luminescence at indicated photon energies under excitation by amplified pulses at a wavelength of 790 nm. The ordinate is in a unit proportional to photons per second per unit energy interval. The intensity becomes larger toward longer wavelength in infrared.

Figure 2(b) shows the normalized luminescence intensity in a wider energy range from 1.3 to 0.23 eV. As the band dispersion is symmetric about the crossing point, this corresponds to the range from 0.65 to 0.115 eV for kinetic energy of electron or hole. The luminescence signal has always a spikelike component near $t = 0$. The dashed curve is the cross correlation traces between the gating pulse and the pumping pulse reflected by the sample surface. As shown in Fig. 2(b), the rising part is mostly the same at all photon energies, and close to the cross-correlation trace (dashed curve). This indicates that the carriers are scattered to whole energy range of the band in a very short time.

The decay profiles show clear energy dependence; the time constant increases as the photon energy decreases [inset of Fig. 2(b)]. This behavior reflects the cooling process of the carriers, as seen in the transient absorption.[13] The existence of very fast carrier relaxation with time constants 13 fs and 100 fs has been reported above 1.2 eV in transient absorption

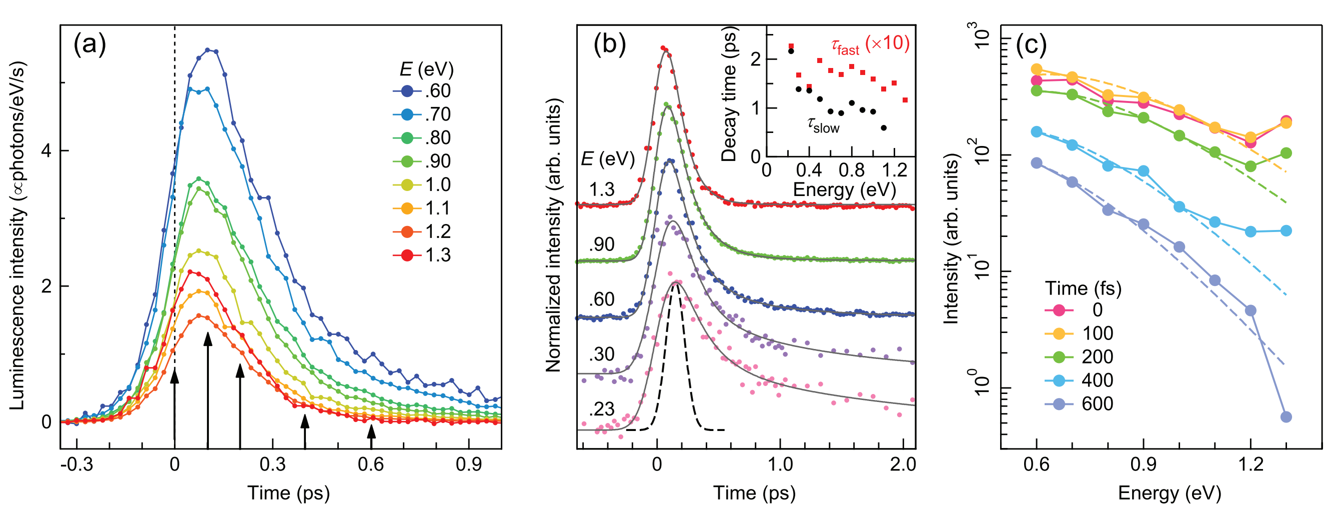

FIG. 2. (Color online) (a) Time evolutions of the luminescence intensities $L(E)$ from 0.6 to 1.3 eV in graphite. The intensities are shown in units proportional to photons/eV/s. The arrows indicate the positions, where the time resolved spectra are constructed in Fig. 1(c). (b) shows the normalized time evolution curves in a wider photon energy range down to 0.23 eV. Dots are the experimental results and the gray curves are the calculated ones resulting from the cooling model described by Eqs. (2) and (3). The dashed black curve is the instrumental function evaluated by cross correlation of the pump and gate pulses. The inset shows the time constants of the fast and slow components evaluated with a phenomenological double exponential fitting. The dotted curves in (c) are the time resolved spectra in a logarithmic scale evaluated at time positions indicated by arrows in (a). The ordinate scale is proportional to photons/eV/s. The dashed curves indicate the calculated luminescence spectra based on the Fermi-Dirac distribution.

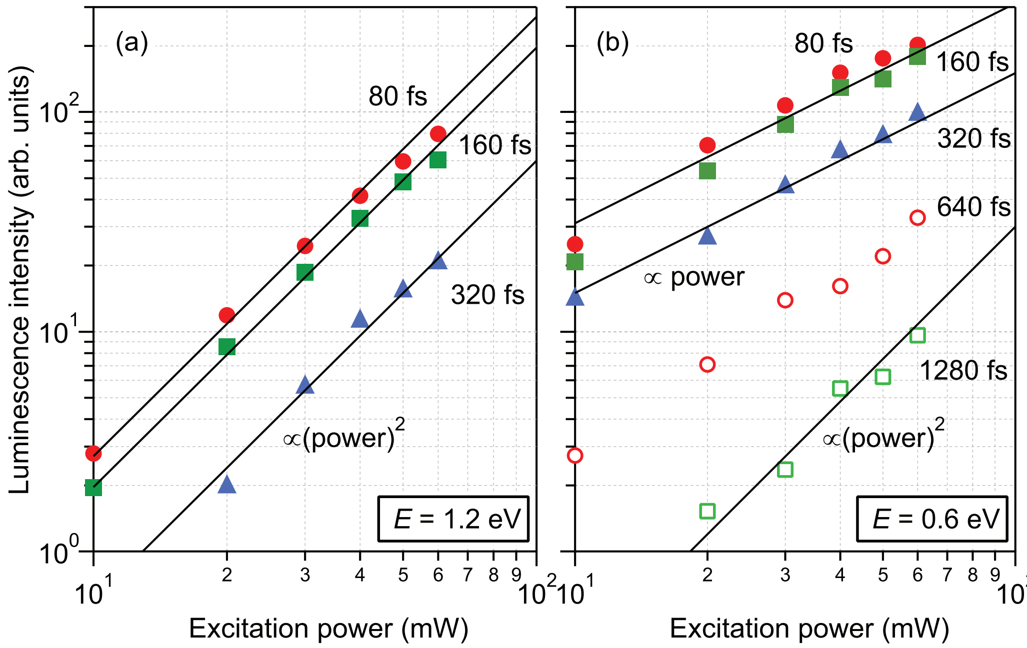

FIG. 3. (Color online) Excitation power dependence of luminescence intensity at several delay times. (a) and (b) show the results for 1.2 eV and 0.6 eV, respectively. The black straight lines correspond to square and linear dependences.

measurements.[13] As we observe the electrons in lower energy, the apparent time constants (180 fs and 1 ps at 0.8 eV) are larger than these values [see inset of Fig. 2(b)].

The time-resolved spectra are constructed from the data in Fig. 2(a) and shown in Fig. 2(c) in a logarithmic scale. The intensity is higher at the lower-energy side reflecting the thermalized carrier distribution. The spectral weight moves to the lower-energy side as time elapses, reflecting the cooling process. Until 200 fs, the intensities at 1.3 eV are larger than that at 1.2 eV, reflecting nonthermalized carrier distribution, which will be discussed later.

To analyze the time evolution of the luminescence spectra, we use a Fermi-Dirac distribution $f(E_e,T_e)$ and $f(E_h,T_h)$ for electrons and holes at temperatures T_e and T_h, respectively [see Fig. 1(b)];

$$f(E_{e,h},T_{e,h}) = 1/[\exp(E_{e,h} - \mu_{e,h})/k_BT + 1]. \tag{1}$$

Here, $\mu_{e,h}$ are the chemical potentials of electron and hole systems. The luminescence intensity at a photon energy E is given by

$$L(E) = WE^3 D_e(E/2) f_e(E/2,T_e) D_h(E/2) f_h(E/2,T_h), \tag{2}$$

where W is a constant determined by a dipole transition matrix. As we observe a spontaneous emission, the factor E^3 is introduced. $D_{e,h}$ are the density of state of electrons and holes given by

$$D_{e,h}(E) \propto |E_{e,h}|. \tag{3}$$

As shown by Eq. (2), the instantaneous luminescence intensity at E will be proportional to a product of $f_e(E/2,T_e)$ and $f_h(E/2,T_h)$. On the other hand, the corresponding PES signal at $E/2$ is given by

$$P(E/2) \propto D_e(E/2) f_e(E/2,T_e). \tag{4}$$

The excitation power dependence of the luminescence intensity at fixed photon energies and delay times are shown in Fig. 3. Here, the fluence is estimated to be 2×10^{21} photons/cm^3 at 10 mW. The intensities of 1.2 eV luminescence show nearly square dependencies as expected from Eq. (2). This behavior is typical for free carrier recombination luminescence in undoped semiconductors.[19] We should note that we observe an instantaneous luminescence intensity rather than the time-integrated one, which is often discussed in steady-state luminescence measurements, where the exciton effects and competition between radiative and nonradiative processes largely modifies the power dependence.[20]

In contrast, the slope for 0.6 eV luminescence at the early stage (80, 160, 320 fs) have nearly linear power dependence [Fig. 3(b)]. This means that the carrier distribution at the relevant energy does not increase in proportion to the input fluence. If the cooling is delayed due to hot phonon effect, the carrier population at 0.3 eV (1/2 of 0.6 eV), will be more suppressed at higher fluence. Even at this photon energy, the slope increases at larger delay time and approaches to square dependence at 1280 fs.

The hot phonon effect in graphene was discussed by Butscher *et al.*,[21] based on density matrix theory considering electron-phonon energy transfer and subsequent decay of the phonons. The results show that the cooling of the electrons drastically slows down after 20 fs and considerable population is accumulated above 0.3 eV mainly due to the hot phonon effect, that is, the temperature of Γ-phonon mode becomes higher due to energy supply from the electron system. After 40 fs the electron distribution begins to approach the ordinary

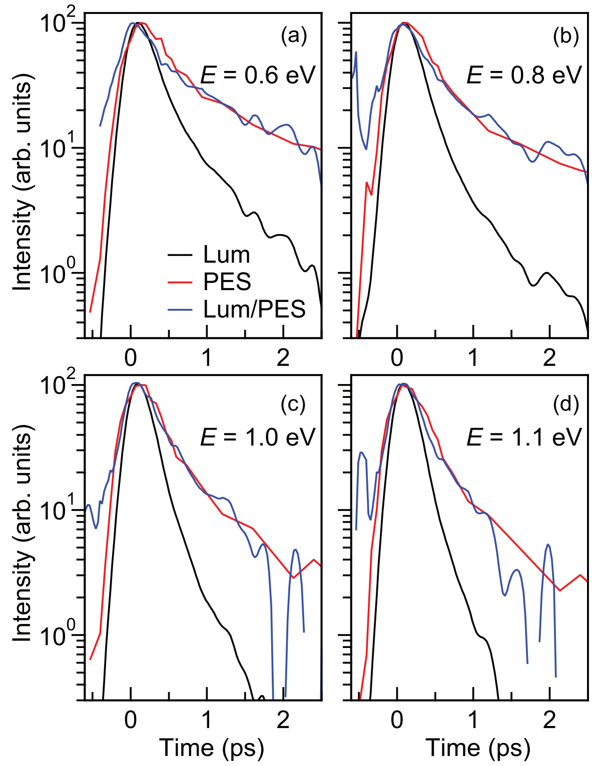

FIG. 4. (Color online) (a)–(d) show time evolution curves for luminescence (black), photoemission (red) and ratio of these two curves (blue), which denotes the hole dynamics. Vertical positions are adjusted for a convenient comparison. TrPES data (1.48 eV pumping pulses and 5.9 eV probe pulses at a repetition frequency of 250 kHz; overall resolution was 400 fs) were compiled from the supporting information of Ref. 12.

Fermi-Dirac distribution. However, the hot phonon population persists still at 500 fs and hinders the electron population at lower energies under high fluence.

In order to separate the dynamics of electron and hole systems, we use the information from TrPES measurements. The angle-integrated PES signal has been taken with an averaged pumping power of 78 mW at 1.48 eV.[12] The red curves in Figs. 4(a)–4(d) are the recompiled data shown in supporting information of Ref. 12. and show the decay profiles of the photoelectron signal at $E/2$ (measured from E_F).

As the hole distribution is proportional to the ratio of Eqs. (2) and (4), we obtain

$$f_h(E/2,T_h)D_h(E/2) \propto L(E)/P(E/2)/E^3. \qquad (5)$$

The comparison is made for time evolution curves at various energies in Figs. 4(a)–4(d).

The black curves show the luminescence intensity at E, which reflect the product of the electron distribution at $E/2$ and hole distribution at $-E/2$. Here, the curves are convoluted with a Gaussian function to mimic the comparable time resolution as TrPES curves. As Eq. (5) indicates, the decay profiles of the hole concentration can be obtained by taking the ratio of these two curves, which are shown by blue curves. As can be seen from the plots, the curves for electrons and holes are in very good agreement between $E = 0.6$ and 1.1 eV. From this comparison, the symmetric behavior of electrons and holes is *experimentally* shown rather than an *assumption*.

Then we can now set

$$f_h(E/2,T_h) = f_e(E/2,T_e) \qquad (6)$$

and

$$T_h = T_e. \qquad (7)$$

As the distribution of electrons and holes are symmetric, we set

$$\mu_h = -\mu_e, \qquad (8)$$

as has been done in Ref. 13. In this literature, it was shown that the chemical potential of electron and hole was different at very early stage (typically <200 fs), and single chemical potential is established at a later time. In TrPES experiments also it is shown that the Fermi-Dirac distribution with a single chemical potential is appropriate after 200 fs.[12] As we treat the phenomena only after 200 fs, we can safely assume $\mu_h = \mu_e = 0$.

The time-resolved spectra in Fig. 2(c) are well fitted by Eq. (2) with appropriate electron (hole) temperature $T_e(t)$ $[=T_h(t)]$ and $\mu = 0$ for each instance as shown by dashed curves. The experimental data points at 1.3 eV before 200 fs are considerably higher than the curve derived from Eq. (2) at early stage. This shows the existence of nonthermalized carriers. This is very similar to the case of a narrow gap semiconductor, InAs, where the nonthermalized component was found as a hump in the time-resolved luminescence spectrum.[22] It should be noted that the Fermi-Dirac analysis is applicable in the energy region sufficiently lower than the excitation photon energy. The time evolution of the electron temperature $T_e(t)$ determined in this way is plotted in Fig. 5. Here, the fitting analysis was performed for the data after 200 fs.

We tried to fit this curve with a double exponential function,

$$T_e = T_1 \exp(-t/\tau_1) + T_2 \exp(-t/\tau_2) + T_{\mathrm{RT}} \qquad (9)$$

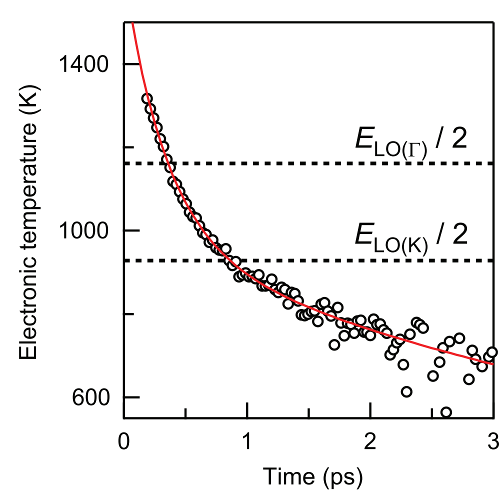

FIG. 5. (Color online) Shown is the carrier temperature deduced from the fitting of the spectral shape defined by Eqs. (2), (6) and (7) to the time-resolved luminescence spectra (open circles). The black line shows the calculated result of the cooling model defined by Eq. (3). The dotted horizontal lines show one half of the LO(Γ) and LO(K) phonon energies converted to temperature scale.

Here, $T_{RT} = 297$ K is the room temperature, while T_1 and T_2 are phenomenological fitting parameters. The electron temperature shown in Fig. 5 is well reproduced with $T_1 = 641$ K, $T_2 = 683$ K, $\tau_1 = 0.35$ ps, and $\tau_2 = 5.16$ ps. The fast component τ_1 is very short compared to those in ordinary semiconductors. This seems to correspond to the reported fast decay component of transient absorption.[13]

This indicates existence of a very efficient energy dissipating mechanism. The optical phonons (LO at Γ and K) in graphite at Γ point have exceptionally high energies, 200 meV (five times of that in GaAs) and 160 meV, respectively,[23] which mediate efficient cooling of carriers. Another important factor is the absence of energy gap. This enables cooling with phonon emission across the Fermi energy, in other words, electron-hole recombination accompanying phonon emission [see Fig. 1(a)]. This situation is contrasted with ordinary semiconductors. For example, in InSb, which is known as a narrow gap semiconductor,[24] the gap energy (0.18 eV) is still eight times larger than the highest-energy optical phonon (23 meV), resulting in a long-lived luminescence.[25] However, when T_e becomes lower than one half of the phonon energy ($E_{\mathrm{LO}(\Gamma)}/2$ and $E_{\mathrm{LO(K)}}/2$), this process will be suppressed, resulting in a slower cooling rate.

Dynamics in the very low energy region below 0.12 eV (optical transition energy) have been studied by using a transient terahertz wave absorption spectroscopy[14] and an efficient transfer of the electronic energy to coupled optical phonon (COP) modes and a slow energy transfer from the COP modes to entire phonon system have been revealed. This corresponds to the last stage of the relaxation, which proceeds in the picosecond region. The slower component ($\tau_2 = 5.16$ ps) observed in luminescence is in reasonable agreement with the reported value 7 ps for the decay constant of electron temperature.[14]

We speculate the slower (τ_2) cooling process corresponds to the energy dissipation of electrons mediated by acoustic phonons, because the crossover of the slope occurs around the electron temperature close to one half of the optical phonon energy.

IV. CONCLUSION

In conclusion, we observed the infrared recombination luminescence in graphite and successfully extracted the hole dynamics by using the time-evolution data of luminescence and photoemission. Thus we have shown experimentally that the behaviors of electrons and holes in graphite are nearly symmetric. We propose this luminescence-photoelectron combined experiment as a methodology for investigating hole dynamics, being applicable to doped/undoped graphenes and other luminescent materials.

ACKNOWLEDGMENTS

This work was supported by a Grant-in-Aid for Scientific Research (A) (Grant No. 23244063) and partly supported by the Grant-in-Aid for Scientific Research (Grant No. 23740256) from the Ministry of Education, Culture, Sports, Science, and Technology of Japan.

[1] W. S. Fann, R. Storz, H. W. K. Tom, and J. Bokor, Phys. Rev. B **46**, 13592 (1992).
[2] L. Perfetti, P. A. Loukakos, M. Lisowski, U. Bovensiepen, H. Eisaki, and M. Wolf, Phys. Rev. Lett. **99**, 197001 (2007).
[3] J. Azuma, K. Takahashi, and M. Kamada, Phys. Rev. B **81**, 113203 (2010).
[4] J. Graf, C. Jozwiak, C. L. Smallwood, H. Eisaki, R. A. Kaindl, D.-H. Lee, and A. Lanzara, Nature Phys. **7**, 805 (2011).
[5] E. Papalazarou, J. Faure, J. Mauchain, M. Marsi, A. Taleb-Ibrahimi, I. Reshetnyak, A. van Roekeghem, I. Timrov, N. Vast, B. Arnaud, and L. Perfetti, Phys. Rev. Lett. **108**, 256808 (2012).
[6] K. S. Novoselov, A. K. Geim, S. V. Morozov, D. Jiang, Y. Zhang, S. V. Dubonos, I. V. Grigorieva, and A. Firsov, Science **306**, 666 (2004).
[7] C. Berger, Z. Song, X. Li, X. Wu, N. Brown, C. Naud, D. Mayou, T. Li, J. Hass, A. N. Marchenkov, E. H. Conrad, P. N. First, and W. A. de Heer, Science **312**, 1191 (2006).
[8] A. K. Geim and K. S. Novoselov, Nature Mater. **6**, 183 (2007).
[9] S. Y. Zhou, G.-H. Gweon, J. Graf, A. V. Fedorov, C. D. Spataru, R. D. Diehl, Y. Kopelevich, D.-H. Lee, S. G. Louie, and A. Lanzara, Nature Phys. **2**, 595 (2006).
[10] P. R. Wallace, Phys. Rev. **71**, 622 (1947).
[11] G. Moos, C. Gahl, R. Fasel, M. Wolf, and T. Hertel, Phys. Rev. Lett. **87**, 267402 (2001).
[12] Y. Ishida, T. Togashi, K. Yamamoto, M. Tanaka, T. Taniuchi, T. Kiss, M. Nakajima, T. Suemoto, and S. Shin, Sci. Rep. **1**, 64 (2011).
[13] M. Breusing, C. Ropers, and T. Elsaesser, Phys. Rev. Lett. **102**, 086809 (2009).
[14] T. Kampfrath, L. Perfetti, F. Schapper, C. Frischkorn, and M. Wolf, Phys. Rev. Lett. **95**, 187403 (2005).
[15] C. H. Lui, K. F. Mak, J. Shan, and T. F. Heinz, Phys. Rev. Lett. **105**, 127404 (2010).
[16] T. Koyama and T. Suemoto, Rep. Prog. Phys. **74**, 076502 (2011).
[17] Y. Takahashi, H. Kitagawa, and T. Suemoto, Phys. Rev. B **79**, 153103 (2009).
[18] K. Yasukawa, Y. Takahashi, T. Suemoto, and S. Kurita, J. Phys. Soc. Jpn. **76**, 084707 (2007).
[19] See, for example, P. Yu and M. Cardona, *Fundamentals of Semiconductors* (Springer-Verlag, Berlin, 1996), Chap. 7, p. 339.
[20] T. Schmidt, K. Lischka, and W. Zulehner, Phys. Rev. B **45**, 8989 (1992).
[21] S. Butscher, F. Milde, M. Hirtschulz, E. Malic, and A. Knorr, Appl. Phys. Lett. **91**, 203103 (2007).
[22] H. Nansei, S. Tomimoto, S. Saito, and T. Suemoto, Phys. Rev. B **59**, 8015 (1999).
[23] D. D. L. Chung, J. Mater. Sci. **37**, 1475 (2002).
[24] Springer Materials, The Landort-Bernstein Database, http://www.springermaterials.com.
[25] T. Suemoto, S. Sakaki, and M. Nakajima (unpublished).